A&A manuscript no.
(will be inserted by hand later)

Your thesaurus codes are:
07 (07.05.1, 07.03.1, 03.13.6, 10.19.1)

ASTRONOMY
AND
ASTROPHYSICS
1.2.2008

The "human" statistics of terrestrial impact cratering rate⋆

L. Jetsu

NORDITA, Blegdamsvej 17, Copenhagen 2100, Denmark

Received; accepted

Abstract. The most significant periodicities in the terrestrial impact crater record are due to the "human–signal": the bias of assigning integer values for the crater ages. This bias seems to have eluded the proponents and opponents of real periodicity in the occurrence of these events, as well as the theorists searching for an extraterrestrial explanation for such periodicity. The "human–signal" should be seriously considered by scientists in astronomy, geology and paleontology when searching for a connection between terrestrial major comet or asteroid impacts and mass extinctions of species.

Key words: Solar system: Earth – Comets, Techniques: statistical, Galaxy: solar neighbourhood

1. Introduction

An outstanding series of papers appeared in 1984 when a 28.4 Myr cycle was detected in the terrestrial impact crater record (Alvarez & Muller 1984, Davis et al. 1984, Whitmire & Jackson 1984). This value was close to the 26 Myr cycle discovered in the geological record of major mass extinctions of species (Raup & Sepkoski 1984). The fascinating idea of periodic comet impacts causing ecological catastrophies emerged (Alvarez & Muller 1984, Davis et al. 1984). It was suggested that an unseen solar companion (Nemesis) might induce gravitational disturbances to the Oort comet cloud triggering periodic cometary showers (Davis et al. 1984, Whitmire & Jackson 1984). Other astronomical models have been proposed later to account for the above periodicities, the "galactic carrousel" being perhaps the most widely accepted model (e.g. the review by Rampino & Haggerty 1996, and references). The main idea of the "galactic carrousel" model is that the Oort comet cloud is periodically perturbed by galactic tides as the Solar System revolves around the centre of the Milky Way galaxy.

We will show that only one extremely significant regularity exists in the impact crater record: the "human–signal".

2. Data

We chose $n = 82$ impact craters with a diameter D_i [km] and an age t_i [Myr], which had an error (σ_{t_i}) in the database maintained by the Geological Survey of Canada.[1] These data are *only* published in electronic form in our Table 1. Eight simultaneous events were combined ($\Rightarrow n = 74$) with the relations $\sigma_{1,2} = \min[\sigma_{t_1}, \sigma_{t_2}]/\sqrt{2}$ and $D_{1,2} = (D_1^2 + D_2^2)^{1/2}$, where σ_{t_1}, σ_{t_2}, D_1 and D_2 refer to the individual events. The geographical coordinates of these pairs imply an occurrence of a double impact, except for one pair ($i = 37$). Combining probable double impacts leaves our result unchanged, but provides better statistics. Six subsamples were selected from Table 1 ($n = 74$):

C1: $5 \leq t$
C2: $t \leq 250$, $\sigma_t \leq 20$, $D \geq 5$
C3: $5 \leq t \leq 300$, $\sigma_t \leq 20$
C4: C1, t is not a multiple of 5
C5: C2, t is not a multiple of 5
C6: C3, t is not a multiple of 5

Criteria similar to C2 and C3 have been applied earlier (Grieve & Pesonen 1996, Matsumoto & Kubotani 1996). We also analysed the sample (C7: $n = 13$), where the 28.4 Myr cycle was originally detected (Alvarez & Muller 1984), and one sample of mass extinctions of species (C8: n=8), recently compared to the impact crater record (Matsumoto & Kubotani 1996). Two sets of weights were derived:

$$w_{t_i} = A_t\ \sigma_{t_i}^{-2} \text{ and } w_{D,i} = A_D\ D_i,$$

where the constants $A_t = n/[\sum_{i=1}^{n} \sigma_i^{-2}]$ and $A_D = n/[\sum_{i=1}^{n} D_i]$ ensure that $\sum_i^n w_{t_i} = \sum_i^n w_{D_i} = n$. The two largest ($w_{max,1}$, $w_{max,2}$) and the smallest (w_{min}) weights, the ratio $W_R = w_{max,1}/w_{min}$ and the average $s = (w_{max,1} + w_{max,2})/2$ for C1, ..., C7 are given in Table 2 (No σ_{t_i} were available for C8).

3. Analysis

Two types of techniques have been mainly applied to search for periodicity in the impact crater record: the power spectrum method and those discussed by Yabushita (1991). The 28.4 Myr cycle was detected with the former technique (Alvarez & Muller 1984). Techniques of the latter type have been applied, e.g. by Yabushita (1991) and Grieve & Pesonen (1996). Yet it has not been fully realized that these techniques are most sensitive to uni–modal phase distributions. These phases are *circular* data: a random sample of measurements representing ϕ_i at t_i folded with a period P (i.e. $\phi_i = \mathrm{FIX}[t_i/P]$, where FIX removes the integer part of t_i/P). Several nonparametric methods for detecting both uni– and multi–modal ϕ_i distributions

Send offprint requests to: L. Jetsu (jetsu@nordita.dk)

⋆Table 1 is only available in electronic form: see editorial in A&A 1992, Vol 266, page E1

[1] //gdcinfo.agg.emr.ca/cb-bin/crater/crater_table?e

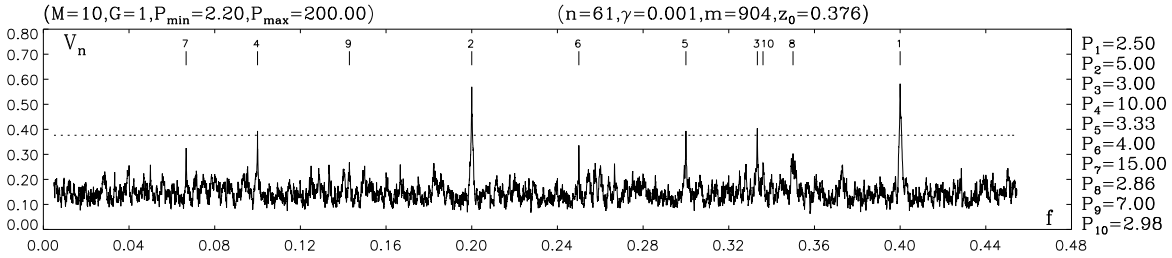

Fig. 1. The ten best period candidates detected with the K–method for C_1 with $n=61$: the overfilling factor (Jetsu & Pelt 1996: Eq. 12) is $[\Delta\phi]^{-1}=GM=10$ for this test between $P_{\rm min}=2.2$ and $P_{\rm max}=200$. The statistics for $m=904$ independent frequencies yield the level $P(V_{\rm n}\geq z_0)=\gamma=0.001$ outlined with a horizontal line. The numbers above the short vertical lines denote the locations of $P_1,...,P_{10}$.

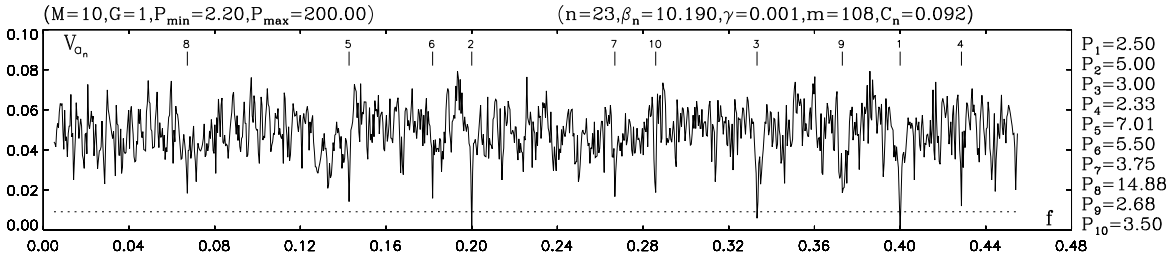

Fig. 2. The ten best period candidates detected with the WSD–method for $C_6(w_{\rm D})$ with $n=23$: the level $P(V_{a_{\rm n}}\leq C_{\rm n}/\beta_{\rm n})=\gamma=0.001$ for $m=108$ is outlined with a horizontal line ($P_{\rm min}$, $P_{\rm max}$, G and M as in Fig. 1).

Table 2. The weights $w_{\rm t}$ and $w_{\rm D}$ of C_1, ..., C_7: the two largest ($w_{\rm max,1}$, $w_{\rm max,2}$) and the smallest ($w_{\rm min}$) weights, the ratio $W_{\rm R}=w_{\rm max,1}/w_{\rm min}$, the average $s=(w_{\rm max,1}+w_{\rm max,2})/2$, and the breakdown parameter $R(s)$ (Jetsu 1996: Eq. 5).

w	n	$w_{\rm min}$	$w_{\rm max,1}$	$w_{\rm max,2}$	$W_{\rm R}$	s	$R(s)$
$C_1(w_{\rm t})$	61	$3.15\cdot10^{-6}$	50.41	6.43	$1.60\cdot10^{7}$	28.42	3.57
$C_1(w_{\rm D})$	61	$4.44\cdot10^{-2}$	8.32	6.93	187.50	7.63	0.10
$C_2(w_{\rm t})$	34	$2.75\cdot10^{-5}$	27.54	4.41	$1.00\cdot10^{6}$	15.97	4.21
$C_2(w_{\rm D})$	34	0.15	4.66	2.74	30.91	3.70	0.10
$C_3(w_{\rm t})$	35	$1.81\cdot10^{-4}$	29.00	3.70	$1.60\cdot10^{5}$	16.35	3.94
$C_3(w_{\rm D})$	35	$6.99\cdot10^{-2}$	4.75	2.80	68.00	3.77	0.10
$C_4(w_{\rm t})$	27	$1.16\cdot10^{-4}$	22.44	2.86	$1.94\cdot10^{5}$	12.65	4.14
$C_4(w_{\rm D})$	27	$6.47\cdot10^{-2}$	6.26	3.55	96.77	4.91	0.23
$C_5(w_{\rm t})$	25	$2.03\cdot10^{-5}$	20.26	3.24	$1.00\cdot10^{6}$	11.75	4.30
$C_5(w_{\rm D})$	25	0.15	4.66	2.74	30.91	3.70	0.17
$C_6(w_{\rm t})$	23	$1.20\cdot10^{-4}$	19.15	2.44	$1.60\cdot10^{5}$	10.80	4.23
$C_6(w_{\rm D})$	23	$8.17\cdot10^{-2}$	4.48	2.63	54.84	3.56	0.19
$C_7(w_{\rm t})$	13	$1.09\cdot10^{-2}$	8.90	1.09	816.33	4.99	1.41
$C_7(w_{\rm D})$	13	0.15	2.94	2.36	20.00	2.65	0.33

exist. We applied two such methods by Kuiper (1960: the K–method) and Swanepoel & De Beer (1990: the SD–method), and their weighted versions (Jetsu & Pelt 1996: the WK– and the WSD–methods), which can utilize the additional information in $w_{\rm t}$ and $w_{\rm D}$. Our notations are as in Jetsu & Pelt (1996).

The limit $t\geq5$ eliminates a bias (C_1, C_3, C_4 and C_6), because over 17 % of $t_{\rm i}$ in Table 1 are below this limit, e.g. these $t_{\rm i}$ have $\phi_{\rm i}\leq0.05$ for $P\geq100$. A limit in t is unnecessary for C_2 and C_5, since the criteria in $\sigma_{\rm t}$ and D eliminate most of the $t_{\rm i}\leq5$. The criterion in D was applied, because earlier studies have indicated different periodicities for $t_{\rm i}$ of larger and smaller craters (e.g. Yabushita 1991).

The statistical "null hypothesis":

H_0: "The $\phi_{\rm i}$ of $t_{\rm i}$ with an arbitrary period P are randomly distributed between 0 and 1."

was tested. All tests were performed between $P_{\rm min}=2.2$ and $P_{\rm max}=200$. The preassigned significance level for rejecting H_0 was $\gamma=0.001$. Two examples of these tests are displayed in Figs. 1 and 2. Most of the detected P reaching $\gamma=0.001$ are integers or ratios of two integers (see Table 3). We call this regularity arising from the bias of assigning integer values for $t_{\rm i}$ as the "human–signal". Unfortunately, any arbitrary P can be expressed by a ratio of two integers. Two P_1 and P_2 of the "human–signal" will induce a set of spurious periods $P'=[P_1^{-1}+k_1(k_2P_2)^{-1}]^{-1}$ ($k_1=\pm1,\pm2,...$ and $k_2=1,2,...$). Furthermore, another set of spurious periods will be $P'=k_3P_1P_2$ ($k_3=1,2,...$). The "human–signal" is strongest in C_1, since many larger $t_{\rm i}$ end with 5 or 0, hence C_4, C_5 and C_6 were selected. An arbitrary $P_{\rm min}=2.2$ was chosen to avoid the detection of, e.g. $P=2$, 3/2, and 1. Note that the order of significance for the period candidates in Figs. 1 and 2 is not necessarily the same as in Table 3, since these periodograms were derived for the overfilling factor $[\Delta\phi]^{-1}=GM=10$ (Jetsu & Pelt 1996: Eq. 12). The final values of Table 3 in the vicinity of these period candidates were determined with $[\Delta\phi]^{-1}=100$. The four nonparametric methods are not "equally sensitive" to different types of $\phi_{\rm i}$ distributions (Jetsu 1996, Jetsu & Pelt 1996), which explains the differences in the detected P of Table 3.

Although uncertainties in some critical level estimates $Q_{\rm K}$, $Q_{\rm WK}$, $Q_{\rm SD}$ and $Q_{\rm WSD}$ exist, these do not alter the *order* of significance for the detected P (Jetsu & Pelt 1996). Thus the "human–signal" is the most significant periodicity in the data. Firstly, the estimate for the number of independent frequencies in all tests was $m=(f_{\rm max}-f_{\rm min})/f_0$, where $f_{\rm max}=P_{\rm min}^{-1}$, $f_{\rm min}=P_{\rm max}^{-1}$ and $f_0=(t_{\rm max}-t_{\rm min})^{-1}$. These m estimates were checked with the empirical correlation function $r(k)$ (Jetsu & Pelt 1996: Eq. 14). We denote the number of indepen-

Table 3. The five best periods detected in C$_1$, ..., C$_8$ with the K–, WK–, SD– and WSD–methods: The estimate of the number of independent frequencies is m for a sample of a size n. The symbols ‡ and † denote the cases $m > m'$ and $m < m'$. The critical levels for each period P are $Q_{\rm K}$ $Q_{\rm WK}$ $Q_{\rm SD}$ and $Q_{\rm WSD}$. The rejection of H_0 with $\gamma = 0.001$ is indicated by •. Finally, the cases when an application of some particular method would not yield reliable results are denoted by $*$

	K–method no weights P ($Q_{\rm K}$)	WK–method $w_{\rm D}$ P ($Q_{\rm WK}$)	SD–method no weights P ($Q_{\rm SD}$)	WSD–method $w_{\rm D}$ P ($Q_{\rm WSD}$)
C$_1$	2.50 (~ 0‡) •	2.50 (~ 0‡) •	20.00 (0‡) •	2.22... (0‡) •
$n = 61$	5.00 ($2.0{\cdot}10^{-13}$‡) •	3.00 ($1.0{\cdot}10^{-13}$†) •	2.66... (0‡) •	5.00 (0‡) •
$m = 904$	3.00 ($3.9{\cdot}10^{-6}$‡) •	5.00 ($1.2{\cdot}10^{-8}$†) •	5.00 (0‡) •	2.66... (0‡) •
	10.00 ($2.1{\cdot}10^{-4}$‡) •	15.00 ($5.0{\cdot}10^{-8}$†) •	8.00 (0‡) •	4.00 (0‡) •
	3.33 ($2.1{\cdot}10^{-4}$‡) •	9.97 ($4.1{\cdot}10^{-7}$†) •	2.50 (0‡) •	20.00 (0‡) •
C$_2$	3.00 (0.0078)	2.50 ($2.6{\cdot}10^{-5}$) •	5.00 ($8.9{\cdot}10^{-10}$) •	5.00 ($8.9{\cdot}10^{-10}$) •
$n = 34$	2.50 (0.11)	7.76 ($6.6{\cdot}10^{-4}$) •	2.50 ($8.9{\cdot}10^{-10}$) •	2.50 ($8.9{\cdot}10^{-10}$) •
$m = 110$	11.67 (0.58)	3.00 ($7.4{\cdot}10^{-4}$) •	3.00 ($1.6{\cdot}10^{-9}$) •	3.00 ($1.9{\cdot}10^{-9}$) •
	17.50 (0.62)	9.95 (0.0037)	2.25 ($4.0{\cdot}10^{-9}$) •	6.00 ($6.7{\cdot}10^{-9}$) •
	7.00 (0.73)	12.56 (0.0046)	6.00 ($5.0{\cdot}10^{-9}$) •	4.00 ($7.3{\cdot}10^{-9}$) •
C$_3$	2.50 (0.0023)	2.50 ($1.4{\cdot}10^{-6}$) •	5.00 ($4.2{\cdot}10^{-10}$) •	2.50 ($4.2{\cdot}10^{-10}$) •
$n = 35$	3.00 (0.0053)	3.00 ($1.3{\cdot}10^{-4}$) •	2.66... ($4.2{\cdot}10^{-10}$) •	8.00 ($4.2{\cdot}10^{-10}$) •
$m = 127$	5.00 (0.18)	7.76 ($1.5{\cdot}10^{-4}$) •	2.50 ($4.2{\cdot}10^{-10}$) •	5.00 ($4.2{\cdot}10^{-10}$) •
	2.86 (0.58)	12.56 (0.0016)	4.00 ($4.2{\cdot}10^{-10}$) •	4.00 ($4.2{\cdot}10^{-10}$) •
	11.62 (0.80)	9.95 (0.0038)	10.00 ($4.2{\cdot}10^{-10}$) •	2.66.. ($4.2{\cdot}10^{-10}$) •
C$_4$	2.50 (0.33‡)	2.50 ($2.3{\cdot}10^{-4}$†) •	4.00 ($3.1{\cdot}10^{-6}$‡) •	4.00 ($3.1{\cdot}10^{-6}$‡) •
$n = 27$	13.20 (0.83‡)	2.98 ($5.3{\cdot}10^{-4}$†) •	2.50 ($3.1{\cdot}10^{-6}$‡) •	2.50 ($3.1{\cdot}10^{-6}$‡) •
$m = 904$	3.00 (0.88‡)	2.70 ($6.3{\cdot}10^{-4}$†) •	5.00 ($3.1{\cdot}10^{-6}$‡) •	5.00 ($3.1{\cdot}10^{-6}$‡) •
	2.98 (0.96‡)	7.77 ($7.1{\cdot}10^{-4}$†) •	10.00 ($3.1{\cdot}10^{-6}$‡) •	10.00 ($3.1{\cdot}10^{-6}$‡) •
	5.50 (0.97‡)	30.00 (0.0016†)	3.33... ($3.1{\cdot}10^{-6}$‡) •	3.33... ($3.1{\cdot}10^{-6}$‡) •
C$_5$	2.50 (0.17)	7.77 (0.0011)	2.50 ($2.0{\cdot}10^{-6}$) •	2.50 ($2.0{\cdot}10^{-6}$) •
$n = 25$	17.43 (0.31)	2.98 (0.0011)	5.00 ($2.0{\cdot}10^{-6}$) •	5.00 ($2.0{\cdot}10^{-6}$) •
$m = 110$	7.50 (0.49)	3.71 (0.0033)	3.00 ($3.7{\cdot}10^{-6}$) •	3.00 ($4.9{\cdot}10^{-6}$) •
	3.00 (0.49)	7.11 (0.017)	3.50 ($1.0{\cdot}10^{-5}$) •	3.50 ($1.3{\cdot}10^{-5}$) •
	14.12 (0.52)	2.67 (0.021)	4.00 ($1.7{\cdot}10^{-5}$) •	4.00 ($3.4{\cdot}10^{-5}$) •
C$_6$	14.00 (0.50)	2.98 ($5.7{\cdot}10^{-4}$) •	5.00 ($1.0{\cdot}10^{-5}$) •	5.00 ($1.0{\cdot}10^{-5}$) •
$n = 23$	7.00 (0.56)	7.77 (0.0013)	2.50 ($1.0{\cdot}10^{-5}$) •	2.50 ($1.0{\cdot}10^{-5}$) •
$m = 108$	3.00 (0.61)	3.71 (0.0018)	3.00 ($1.4{\cdot}10^{-5}$) •	3.00 ($1.9{\cdot}10^{-5}$) •
	3.87 (0.69)	13.54 (0.012)	7.00 ($1.9{\cdot}10^{-5}$) •	3.50 ($2.9{\cdot}10^{-5}$) •
	2.50 (0.75)	2.52 (0.013)	3.50 ($2.2{\cdot}10^{-5}$) •	3.75 ($3.8{\cdot}10^{-5}$) •
C$_7$	20.63 (0.083)	*	4.00 (0) •	*
$n = 13$	5.76 (0.11)	*	*	*
$m = 87$	3.82 (0.11)	*	*	*
	2.30 (0.12)	*	*	*
	2.95 (0.12)	*	*	*
C$_8$	2.76 (0.0031)	*	*	*
$n = 8$	3.68 (0.064)	*	*	*
$m = 105$	3.22 (0.13)	*	*	*
	11.03 (0.31)	*	*	*
	13.80 (0.39)	*	*	*

dent frequencies implied by $r(k)$ with m'. Some tests had $m' \neq m$. The correct values for the critical level are smaller when $m > m'$ (i.e. the significance is higher), while the case is opposite for $m < m'$. This problem is only present in C$_1$ and C$_4$ containing less older than younger craters, and thus the inverse of $t_{\rm max} - t_{\rm min}$ provides a poor f_0 estimate. Secondly, $Q_{\rm K} \geq Q_{\rm WK}$ when the same period is detected with the K– and WK–methods (Jetsu & Pelt 1996: Eq. 30), which is due to the large scatter in $w_{\rm D}$ (see Table 2). For example, the sum of the two largest $w_{\rm D}$ in C$_1$($n = 61$) is 15.25, which disrupts the statistics of the WK–method. However, the values of $Q_{\rm K}$ are reliable when $m = m'$. Thirdly, the statistics of the WSD–method are quite robust even for a higher scatter of weights. But the values of $Q_{\rm SD}$ are $Q_{\rm WSD}$ are uncertain for smaller samples, since the analytical estimate for the critical parameter $C_{\rm n}$ is accurate only for larger samples (Jetsu & Pelt 1996: Eq. 16). The SD–method reveals some bizarre cases ($Q_{\rm SD} = 0 \equiv$ never), e.g. for C$_7$ with $P = 4$. No random sample can contain so many time differences that are multiples of 4. Even if C$_7$ contained a period that is apparently not due to the "human–signal", such as the 28.4 Myr (Alvarez & Muller 1984), it is impossible to decide whether this period is a multiple of, say 7x4. In fact, $P = 28.79$ ($Q_{\rm K} = 0.13$) is the sixth most significant period detected with the K–method in C$_7$.

Table 2 shows, why no results for w_t were obtained. The largest w_t are typically $\gtrsim n/2$, and thus the statistics of the WK–method would be unreliable. As for the WSD–method, we refer to the breakdown parameter $R(s)$ in Table 2. If $R(s)$ exceeds unity, the statistics of the WSD–method are disrupted (Jetsu 1996: Eq. 5). Table 2 indicates that the WK– and WSD–methods must not be applied with w_t. Because the high scatter in w_t prevents applications of the WK– and WSD–methods, we checked, if the removal of less accurate t_i would significantly alter $w_{max,1}$ or $R(s)$ for w_t. But this removal of less accurate t_i did not yield $R(s)<1$ for w_t even if this procedure was carried out until only 5 values remained in C_1, ..., C_7. The same applies to $w_{max,1}$, which remains too close to n.

Why was the "human–signal" not detected earlier, while the 28.4 Myr cycle was detected? The answer to the first question is that the ϕ_i distributions connected to the "human–signal" are mostly multi–modal, and can not be detected with methods sensitive to uni–modal ϕ_i distributions. There are several answers to the second question. The 28.4 Myr cycle, as well as any other noninteger period, may be induced by the "human–signal". For example, one earlier study revealed mainly multiples of 5 (Yabushita 1991: e.g. 30x1 =15x2= 10x3 = 6x5). Since C_7 has $Q_{SD}=0$ for $P=4$, no Monte Carlo simulation will ever "succeed" in producing so many exactly equal time differences, let alone the two additional equal t values in C_7, i.e. the earlier significance estimates were not correct (Alvarez & Muller 1984). Finally, the scatter of w_t in C_7 is so large that the case $n=13$ does not occur, because the sum of the two largest w_t is 9.0. An analysis of the superimposed gaussians of these t_i detects periods from the highest peaks with large w_t, while the smaller w_t do not influence the result (e.g. $w_{min}=0.01$).

The small sample C_8 could only be reliably analysed with the K–method. No signs of the 26 Myr cycle were detected (Raup & Sepkoski 1984, 1986), nor any period with $Q_K \leq \gamma = 0.001$. The best periods do not betray any trivial signature of the "human–signal", although half of the t_i are integers. If the most significant $P=2.76$ ($Q_K=0.0031$) represents real periodicity, Raup & Sepkoski (1984, 1986) have identified about every tenth mass extinction event.

4. Conclusions

A few topics must be emphasized to avoid misunderstanding. (I) We did not assume that the integer t_i cause the detected periodicities. On the contrary, the periodicities were uniquely detected with non–parametric statistical methods (i.e. model independent). *We simply tested the "null hypothesis" (H_0) that the impact crater ages represent a random sample of circular data.* The "human–signal" reaches $\gamma=0.001$ in all subsamples C_1, ..., C_7, the critical levels of the SD– and WSD–methods being extremely high. The analytical statistics of our methods are robust, i.e. Monte Carlo or other computational techniques are unnecessary. (II) The "human–signal" induces irregular multi–modal ϕ_i distributions, which were not detected earlier with methods sensitive to uni–modal ϕ_i distributions. For example, the power spectrum method is most sensitive to sinusoidal variations. If the ϕ_i distribution for the "correct" P' were exactly bi–modal, the peaks of the power spectrum would be at P', $P'/2$, ... But the power spectrum method is quite insensitive to more irregular ϕ_i distributions. That the "human–signal" was not detected earlier, over twelve years after the study by Alvarez & Muller (1984), is a direct consequence of favouring methods sensitive to uni–modal ϕ_i distributions. Why should the ϕ_i distributions connected to the possible periodicity in terrestrial impact cratering rate or mass extinctions of species actually be uni–modal or of any regular shape? (III) It may well be that the large σ_{t_i} prevent detection of periodicity (e.g. Heisler & Tremaine 1989). In that case our study is simply an exercise of statistics providing one new argument against real periodicity. However, considering the prevailing theories based on assuming the presence of real periodicities (see e.g. Rampino & Haggerty 1996: "Shiva Hypothesis"), it was a high time to perform this exercise. (IV) The "human–signal" has most probably induced those spurious periods with more or less unimodal ϕ_i distributions, which were detected in several earlier studies (e.g. Alvarez & Muller 1984, Yabushita 1991). In any case, the "human–signal" is clearly the most significant periodicity in the impact crater record. (V) We do not argue that the major comet or asteroid impacts and the mass extinctions of species are uncorrelated, but emphasize that the "human–signal" dominates the time distribution of the former events.

Our conclusions are simple. The epochs of mass extinction events of species may follow a possibly "nonhuman" cycle of 2.76 Myr, but the currently available impact crater data definitely reveals the embarrassing "human–signal". The fellow scientists have unconsciously offered a helping hand to the Nemesis (e.g. Davis et al. 1984) or "galactic carrousel" (e.g. Rampino & Haggerty 1996). The arduous task for the future geological research is to determine more accurate (preferably noninteger) revised ages for impact craters to eliminate the "human–signal", which may then lead to a detection of real periodicity. Over a decade has elapsed in redetecting the regularities of our own integer number system and then interpreting them as periodicity in the ages of impact craters.

Acknowledgements. This work was partly supported by the EC Human Capital and Mobility (Networks) project "Late type stars: activity, magnetism, turbulence" No. ERBCHRXCT940483.

References

Alvarez W., Muller R.A. 1984, Nat 308, 718
Davis M., Hut P., Muller R.A. 1984, Nat 308, 715
Grewing M., Lequeux J., Pottasch S.R. 1992, A&A 266, E1-E2
Grieve R.A.F., Pesonen L.J. 1996, Earth, Moon and Planets 72, 357
Heisler J., Tremaine S. 1989, Icarus 77, 213
Jetsu L., Pelt J. 1996, A&AS 118, 587
Jetsu L. 1996, A&A 314, 153
Kuiper N.H. 1960, Proc. Koningkl. Nederl. Akad. Van Wetenschappen, Series A, 63, 38
Matsumoto M., Kubotani H. 1996, MNRAS 282, 1407
Rampino M.R., Haggerty B.M. 1996, Earth, Moon and Planets 72, 441
Raup D.M., Sepkoski J.J. 1984, Proc. natn. Acad. Sci. USA 81, 801
Raup D.M., Sepkoski J.J. 1986, Sci 231, 833
Swanepoel J.W.H., De Beer C.F. 1990, ApJ 350, 754
Whitmire D.P., Jackson A.A. 1984, Nat 308, 713
Yabushita S. 1991, MNRAS 250, 481

This article was processed by the author using Springer-Verlag LaTeX A&A style file 1990.

Table 1: The ages (t) of the impact craters of a diameter (D) with an error estimate (σ_t) for t. The locations and the values of σ_t and D for the combined events are given in columns 5, 7 and 8, while "Y" denotes the samples C_1, ..., C_6.

i	Crater	Country	t[Myr]	$\sigma_{t_1}/\sigma_{t_2}$	D[km]	D_1/D_2	Location	C_1	C_2	C_3	C_4	C_5	C_6
1	Kaalijärvi	Estonia	0.004±0.001		0.11								
2	Wabar	Saudi Arabia	0.006±0.002		0.097								
3	Boxhole	Australia	0.03±0.0005		0.17								
4	Barringer	U.S.A.	0.049±0.003		1.186								
5	Lonar	India	0.052±0.006		1.83								
6	Pretoria Saltpan	South Africa	0.22±0.052		1.13								
7	Zhamanshin	Kazakhstan	0.9±0.1		13.5				Y			Y	
8	Bosumtwi	Ghana	1.03±0.02		10.5				Y			Y	
9	New Quebec	Canada	1.4±0.1		3.44								
10	Tenoumer	Mauritania	2.5±0.5		1.9								
11	Aouelloul	Mauritania	3.1±0.3		0.39								
12	El'gygytgyn	Russia	3.5±0.5		18				Y			Y	
13	Roter Kamm	Namibia	3.7±0.3		2.5								
14	Bigach	Kazakhstan	6±3		7			Y	Y	Y	Y	Y	Y
15	Shunak	Kazakhstan	12±5		3.1			Y		Y	Y		Y
16	Ries/Steinheim	Germany	15±0.7	(1/1)	24.3	(24/3.8)	N48.9E10.6/N48.0E10.1	Y	Y	Y			
17	Haughton	Canada	23±1		24			Y	Y	Y	Y	Y	Y
18	Logancha	Russia	25±20		20			Y	Y	Y			
19	Popigai	Russia	35±5		100			Y	Y	Y			
20	Chesapeake Bay	U.S.A.	35.5±0.6		85			Y	Y	Y	Y	Y	Y
21	Wanapitei	Canada	37±2		7.5			Y	Y	Y	Y	Y	Y
22	Mistastin	Canada	38±4		28			Y	Y	Y	Y	Y	Y
23	Logoisk	Belarus	40±5		17			Y	Y	Y			
24	Chiyli	Kazakhstan	46±7		5.5			Y	Y	Y	Y	Y	Y
25	Kamensk/Gusev	Russia	49±0.14	(0.2/0.2)	25.2	(25/3.5)	N48.3E40.2/N48.4E40.2	Y	Y	Y	Y	Y	Y
26	Montagnais	Canada	50.5±0.76		45			Y	Y	Y	Y	Y	Y
27	Ragozinka	Russia	55±5		9			Y	Y	Y			
28	Marquez	U.S.A.	58±2		13			Y	Y	Y	Y	Y	Y
29	Chicxulub	Mexico	64.98±0.05		170			Y	Y	Y	Y	Y	Y
30	Kara/Ust-Kara	Russia	73±2.1	(3/3)	69.6	(65/25)	N69.2E65.0/N69.3E65.3	Y	Y	Y	Y	Y	Y
31	Manson	U.S.A.	73.8±0.3		35			Y	Y	Y	Y	Y	Y
32	Lappajärvi	Finland	77.3±0.4		23			Y	Y	Y	Y	Y	Y
33	Boltysh	Ukraine	88±3		24			Y	Y	Y	Y	Y	Y
34	Dellen	Sweden	89±2.7		19			Y	Y	Y	Y	Y	Y
35	Steen River	Canada	95±7		25			Y	Y	Y			
36	Deep Bay/West Hawk	Canada	100±35	(50/50)	13.2	(13/2.44)	N56.4W103.0/N49.8W95.2	Y					
37	Carswell/Zapadnaya	Canada/Ukraine	115±7.1	(10/10)	39.2	(39/4)	N58.4W109.5/N49.7E29.0	Y	Y	Y			
38	Zeleny Gai	Ukraine	120±20		2.5			Y		Y			
39	Mien	Sweden	121±2.3		9			Y	Y	Y	Y	Y	Y
40	Tookoonooka	Australia	128±5		55			Y	Y	Y	Y	Y	Y
41	Romistrovka	Ukraine	140±20		2.7			Y		Y			
42	Gosses Bluff	Australia	142.5±0.5		22			Y	Y	Y	Y	Y	Y
43	Mjølnir	Norway	143±20		40			Y	Y	Y	Y	Y	Y
44	Liverpool	Australia	150±70		1.6			Y					
45	Vepriai	Lithuania	160±30		8			Y					
46	Puchezh-Katunki	Russia	175±3		80			Y	Y	Y			
47	Rochechouart	France	186±8		23			Y	Y	Y	Y	Y	Y
48	Wells Creek/Red Wing	U.S.A.	200±18	(100/25)	15	(12/9)	N36.4W87.7/N47.6W103.6	Y	Y	Y			
49	Manicouagan	Canada	214±1		100			Y	Y	Y	Y	Y	Y
50	Obolon'	Ukraine	215±25		15			Y					
51	Saint Martin	Canada	220±32		40			Y					
52	Araguainha Dome	Brazil	247±5.5		40			Y	Y	Y	Y	Y	Y
53	Kursk	Russia	250±80		5.5			Y					
54	Clearwater West/East	Canada	290±14	(20/20)	44.4	(36/26)	N56.2W74.5/N56.1W74.1	Y		Y			
55	Dobele	Latvia	300±35		4.5			Y					
56	Crooked Creek	U.S.A.	320±80		7			Y					
57	Charlevoix	Canada	357±15		54			Y			Y		
58	Flynn Creek	U.S.A.	360±20		3.55			Y					
59	Siljan	Sweden	368±1.1		52			Y			Y		
60	Kaluga	Russia	380±10		15			Y					
61	Ilyinets	Ukraine	395±5		4.5			Y					
62	La Moinerie	Canada	400±50		8			Y					
63	Couture	Canada	430±25		8			Y					
64	Calvin/Brent	U.S.A./Canada	450±7.1	(10/30)	9.3	(8.5/3.8)	N41.8W86.0/N46.1W78.5	Y					
65	Pilot	Canada	455±2		6			Y					
66	Ames	U.S.A	470±30		16			Y					
67	Gardnos	Norway	500±10		5			Y					
68	Holleford	Canada	550±100		2.35			Y					
69	Mizarai	Lithuania	570±50		5			Y					
70	Jänisjärvi	Russia	698±22		14			Y			Y		
71	Morokweng	South Africa	1400±200		70			Y					
72	Teague	Australia	1630±5		30			Y					
73	Sudbury	Canada	1850±3		250			Y					
74	Vredefort	South Africa	2018±14		300			Y			Y		